

Article

Enhancing Uplink Communication in Wireless Powered Communication Networks Through Rate-Splitting Multiple Access and Joint Resource Optimization

Iqra Hameed ¹, Mario R. Camana ², Mohammad Abrar Shakil Sejan ³ and Hyoung Kyu Song ^{1,*}

¹ Department of Information and Communication Engineering and Convergence Engineering for Intelligent Drone, Sejong University, Seoul 05006, Republic of Korea; engriqrahameed056@gmail.com

² Interdisciplinary Centre for Security, Reliability and Trust, University of Luxembourg, 4365 Luxembourg, Luxembourg; mario.camana@uni.lu

³ Department of Electrical Engineering, Sejong University, Seoul 05006, Republic of Korea; sejan@sejong.ac.kr

* Correspondence: songhk@sejong.ac.kr

Abstract: Wireless powered communication networks (WPCNs) provide a sustainable solution for energy-constrained IoT devices by enabling wireless energy transfer (WET) in the downlink and wireless information transmission (WIT) in the uplink. However, their performance is often limited by interference in uplink communication and inefficient resource allocation. To address these challenges, we propose an RSMA-aided WPCN framework, which optimizes rate-splitting factors, power allocation, and time division to enhance spectral efficiency and user fairness. To solve this non-convex joint optimization problem, we employ the simultaneous perturbation stochastic approximation (SPSA) algorithm, a gradient-free method that efficiently estimates optimal parameters with minimal function evaluations. Compared to conventional optimization techniques, SPSA provides a scalable and computationally efficient approach for real-time resource allocation in RSMA-aided WPCNs. Our simulation results demonstrate that the proposed RSMA-aided framework improves sum throughput by 12.5% and enhances fairness by 15–20% compared to conventional multiple-access schemes. These findings establish RSMA as a key enabler for next-generation WPCNs, offering a scalable, interference-resilient, and energy-efficient solution for future wireless networks.



Academic Editors: Farag M. Sallabi and Mohammad Hayajneh

Received: 7 January 2025

Revised: 4 March 2025

Accepted: 5 March 2025

Published: 6 March 2025

Citation: Hameed, I.; Camana, M.R.; Sejan, M.A.S.; Song, H.K. Enhancing Uplink Communication in Wireless Powered Communication Networks Through Rate-Splitting Multiple Access and Joint Resource

Optimization. *Mathematics* **2025**, *13*, 888. <https://doi.org/10.3390/math13050888>

Copyright: © 2025 by the authors. Licensee MDPI, Basel, Switzerland. This article is an open access article distributed under the terms and conditions of the Creative Commons Attribution (CC BY) license (<https://creativecommons.org/licenses/by/4.0/>).

Keywords: rate-splitting multiple access (RSMA); wireless powered communication networks (WPCNs); wireless energy transfer (WET); wireless information transmission (WIT); sum throughput maximization; fairness optimization; simultaneous perturbation stochastic approximation (SPSA); interference management; energy efficiency; resource allocation

MSC: 94-08; 94-10

1. Introduction

The rapid evolution of 6G networks aims to deliver seamless connectivity, ultra-reliable low-latency communication (URLLC), and enhanced mobile broadband (eMBB), and support massive machine-type communications (mMTC) [1,2]. A crucial aspect of 6G is the integration of low-power Internet of Things (IoT) devices, which will be widely used in applications such as smart cities and industrial automation [3–5]. However, these devices face significant challenges due to limited energy resources. Frequent battery replacement is often impractical, especially for devices deployed in remote or hard-to-reach locations.

This highlights the urgent need for efficient energy management strategies to prolong their operational lifetimes [6,7].

1.1. Wireless Powered Communication Networks

Wireless powered communication networks (WPCNs) offer a promising solution to the energy constraints of low-power IoT devices [8–11]. In WPCNs, devices harvest energy from dedicated power sources, such as energy transmitters (ETs), and use this energy for uplink communication. This eliminates the reliance on frequent battery replacements by leveraging wireless energy transfer. As a result, WPCNs present a sustainable energy solution for low-power IoT devices, making them a viable option for 6G applications [12,13]. However, the performance of a WPCN relies on the coordinated design of energy harvesting and data transmission. Achieving the desired quality of service (QoS) requires optimizing the time allocation between wireless energy transfer (WET) and wireless information transmission (WIT) [14,15]. This allocation directly impacts the network's energy efficiency and overall throughput. In addition, advance applications such as 4K video streaming, virtual reality (VR), and augmented reality (AR) are central to 6G's promise, but these applications demand exceptionally high data rates, low latency, and seamless connectivity [16–18]. VR and AR, in particular, involve immersive experiences where even minor delays or insufficient bandwidth can significantly degrade the user experience. Similarly, 4K video streaming requires stable, high-throughput channels to ensure uninterrupted playback and maintain video quality. To meet these demands, efficient resource allocation strategies in multiple-access channels (MAC) become critical. In 6G networks, multiple-access technologies enable multiple users or devices to share limited communication resources such as frequency, time, or space. These channels ensure the delivery of high data rates to multiple users simultaneously while managing interference and optimizing spectral efficiency.

1.2. Rate-Splitting Multiple Access

Rate-splitting multiple access (RSMA) emerges as a promising candidate to address these challenges in multiple-access networks [19,20]. Unlike traditional multiple-access schemes like time-division multiple access (TDMA) or orthogonal multiple access (OMA), RSMA allows users to split their messages into common and private parts. These parts are transmitted over superimposed signals, enabling the network to manage interference more effectively. RSMA leverages successive interference cancellation (SIC) at the receiver to decode signals in a hierarchical manner, achieving a balance between spectral efficiency and user fairness [21,22]. By allocating power dynamically and managing interference flexibly, RSMA offers the capacity to support the high data rates required by 6G applications while ensuring robust performance in multi-user environments. This integrated design of RSMA and multiple-access technologies establishes the foundation for optimizing energy and information transmission, enabling 6G networks to meet the stringent demands of modern applications.

1.3. Related Works

WPCNs have been extensively studied to address energy constraints in modern communication systems. Significant focus has been placed on throughput maximization by optimizing resource allocation strategies. For instance, Ju et al. proposed a time allocation framework to maximize system throughput by balancing WET and WIT [15]. Energy beamforming, another key aspect, was explored in [23–25], where directional energy transmission enhanced the efficiency of power delivery to devices in WPCNs. In the context of multiple-access techniques, non-orthogonal multiple access (NOMA) has been integrated into WPCNs to improve spectral efficiency [26,27]. Other works include

incorporating hybrid multiple-access schemes, such as the integration of TDMA and FDMA [28], and of NOMA and TDMA [29], to optimize energy and throughput trade-offs in WPCNs. These studies collectively highlight the advancements in WPCNs, focusing on innovative methods to optimize energy efficiency and communication performance in energy-constrained networks. However, no prior research has investigated the performance of WPCNs integrated with RSMA.

RSMA has been widely explored for its ability to optimize spectral efficiency and manage interference in wireless networks. Clerckx et al. laid the foundation of RSMA, showcasing its superiority over traditional multiple-access techniques like NOMA and SDMA in multi-user MISO systems with imperfect channel state information (CSI) [19]. Mao et al. extended this work, demonstrating how RSMA enables simultaneous wireless information and power transfer (SWIPT) in multi-antenna systems, optimizing both communication and energy harvesting performance [30]. Further, Camana et al. explored RSMA in cognitive radio settings, integrating SWIPT to optimize power allocation and beamforming, achieving improved energy and data trade-offs [31]. The integration of RSMA into intelligent reflecting surface (IRS)-assisted SWIPT networks has also been investigated, where dynamic beamforming and rate splitting significantly enhanced energy efficiency and throughput [32].

While most of the early focus was on downlink RSMA, recent studies have highlighted the importance of RSMA in uplink communications. In uplink scenarios, RSMA enables users to transmit their messages in non-orthogonal modes while addressing inter-user interference effectively through message splitting and SIC. Abbasi et al. introduced cooperative RSMA (C-RSMA), leveraging amplify-and-forward relaying and rate-splitting to improve throughput and fairness compared to NOMA [33]. Khisa et al. developed a joint beamforming and power allocation framework for C-RSMA, demonstrating superior SINR and performance over baseline schemes using successive convex approximation (SCA) [34]. Xiao et al. proposed an RSMA-enabled coordinated direct and relay transmission (CDRT) scheme, optimizing power allocation to enhance the reliability and throughput of far users while maintaining fairness for near users [35]. These works highlight uplink RSMA's potential in managing interference and optimizing performance in multi-user networks. Please refer to Table 1 for a summary of the related works.

Table 1. Comparison of existing works and our proposed approach.

Reference	Technique	Objective	Key Limitation	How Our Work Addresses Limitation
[15]	Time allocation in WPCNs	Maximizes throughput by balancing WET and WIT	Does not address interference and fairness issues	Our work integrates RSMA for interference mitigation and fairness enhancement
[24]	Energy beamforming in WPCNs	Improves power transfer efficiency	Limited by multi-user interference and inefficient resource allocation	Our joint optimization of RSMA-based power allocation overcomes these issues
[26]	NOMA-based WPCN	Enhance spectral efficiency	Suffers from high inter-user interference in uplink	RSMA effectively manages interference using rate splitting
[30]	RSMA for SWIPT	Optimizes energy harvesting and data rate trade-offs	Focuses only on downlink RSMA, no uplink extension	Our work extends RSMA to WPCNs in the uplink

Table 1. *Cont.*

Reference	Technique	Objective	Key Limitation	How Our Work Addresses Limitation
[33]	Cooperative RSMA in uplink	Improve fairness and throughput using amplify-and-forward relaying	No consideration of energy harvesting in WPCNs	We integrate RSMA into WPCNs while optimizing energy efficiency
Our Proposed Work	RSMA-aided WPCN	Optimizes throughput, fairness, and energy efficiency	Addresses all limitations above	Joint optimization of RSMA parameters in WPCNs using SPSA

1.4. Motivation and Contributions

Building upon the challenges outlined above regarding the need for efficient resource allocation in WPCNs, this work investigate a key gap in the literature, the integration of advanced multiple-access techniques to optimize both energy transfer and uplink communication. While traditional approaches have been extensively explored, they fall short in terms of flexibly managing interference and ensuring an optimal trade-off between throughput and fairness. RSMA has proven to be an effective approach for interference management and resource allocation in traditional wireless systems. Despite its demonstrated potential in improving throughput and fairness, no prior work has explored the integration of RSMA into WPCNs. The absence of such studies motivated us to investigate how RSMA can enhance WPCN performance by jointly optimizing the energy transfer and uplink communication processes.

The main contributions of this paper are summarized as follows:

- We propose an RSMA-aided WPCN framework for a two-user system, where WET occurs in the downlink and RSMA is applied in the uplink WIT. This design exploits RSMA's interference management capabilities to enhance uplink communication efficiency.
- Two distinct optimization problems are formulated: (a) maximizing the sum throughput to improve overall network efficiency and (b) optimizing fairness to ensure balanced resource allocation among users. These problems are addressed by jointly optimizing the rate-splitting factors and time allocations for the WET and WIT phases. The non-convex nature of these problems is tackled using the simultaneous perturbation stochastic approximation (SPSA) method, which provides an efficient and scalable solution.
- Through comprehensive numerical simulations, we analyze the trade-offs between sum throughput and fairness optimization objectives, providing critical insights into the applicability of RSMA in WPCNs. Our results demonstrate RSMA's potential to achieve balanced performance in energy and communication efficiency, underscoring its relevance for next-generation WPCNs.

2. System Model

In this section, we provide a detailed description of the system model used to analyze the performance of RSMA in a WPCN. As shown in Figure 1, the network comprises a hybrid access point (H-AP) equipped with a single antenna. There are two users, denoted as $\{U_1, U_2\}$, and each is equipped with a single antenna. The system operates in two distinct phases with energy harvesting on the downlink and data transmission on the uplink. The H-AP serves two primary functions by acting as an energy transmitter (ET) in the downlink phase, where it transmits energy signals to the users, allowing them to harvest energy for their uplink data transmission operations, and as a receiver in the uplink phase, where it collects the data transmitted by the users. Users U_1 and U_2 harvest energy

from the H-AP during the downlink phase and then use the harvested energy to transmit their data to the H-AP during the uplink phase.

The communication links between the H-AP and the users, denoted as h_1, h_2 , are modeled using quasi-static, flat-fading channels. The channel coefficients incorporate both large-scale path loss and small-scale fading effects. Specifically, we define the channel coefficient for user U_i as

$$h_i = \frac{g_i}{\sqrt{d_i^\beta}}, \quad i \in \{1, 2\} \quad (1)$$

where g_i represents small-scale fading, d_i is the distance from the H-AP, and β is the path-loss exponent. This formulation explicitly captures the impact of distance on both energy harvesting and uplink transmission. We assume that the channel conditions remain constant during each transmission coherence interval but may vary between different transmission intervals. We assume reciprocal channels, meaning the channel gain remains the same for both downlink and uplink transmissions for each user, which is a reasonable assumption in time-division duplex (TDD) systems. Without loss of generality, we assume that $|h_1|^2 \geq |h_2|^2$. The key system parameters and their descriptions are summarized in Table 2 for clarity.

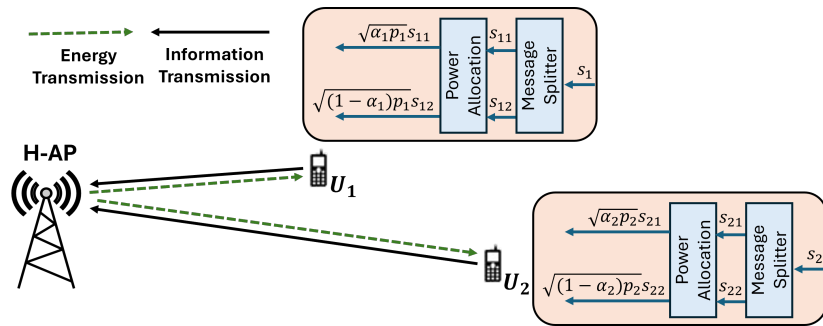


Figure 1. The RSMA-aided wireless powered communication network (WPCN) framework. The hybrid access point (H-AP) first transmits energy to users U_1 and U_2 via wireless energy transfer (WET), followed by wireless information transmission (WIT) in the uplink. Each user employs RSMA, where messages are split into two parts, optimally allocated for power and transmitted to the H-AP.

Table 2. List of parameters and their descriptions.

Symbol	Description	Unit
h_i	Channel coefficient between H-AP and user i	-
P_A	Transmit power at the H-AP	dBm
E_i	Energy harvested by user i	Joules
η_i	Energy conversion efficiency of user i	-
τ_d	Time allocated for downlink energy harvesting	Seconds
τ_u	Time allocated for uplink transmission	Seconds
p_i	Transmit power of user i in uplink	Watts
α_i	Power allocation coefficient for RSMA for user i	-
γ_{ij}	Signal-to-Interference-plus-Noise Ratio (SINR) of stream s_{ij}	-
R_i	Achievable rate of user i	bps/Hz
σ^2	Variance of additive Gaussian noise at H-AP	dBm
$L(x)$	Objective function in optimization problem	-
a_k, c_k	SPSA step size and perturbation constant	-
Δ_k	Perturbation vector in SPSA optimization	-
N	Number of iterations in SPSA algorithm	-

2.1. Phase 1: Downlink Energy Harvesting

During the downlink phase, the H-AP transmits an energy signal with power P_A . The users receive this energy and convert it into usable power through an energy harvesting mechanism. The signal received at U_i is expressed as

$$y_i = \sqrt{P_A}h_i + z_i, \quad i \in \{1, 2\} \quad (2)$$

where z_i represents the noise at U_i during the energy harvesting phase, which is typically negligible due to the high power of the energy signal. The energy harvested by U_i is given by

$$E_i = \eta_i \tau_d P_A |h_i|^2, \quad i \in \{1, 2\} \quad (3)$$

where η_i denotes the energy conversion efficiency of U_i , representing the efficiency of the user's energy harvesting circuitry, and τ_d is the duration of the energy harvesting phase. This harvested energy E_i is stored in the user's battery and will be used during the uplink transmission phase.

2.2. Phase 2: Uplink Data Transmission Using RSMA

In the uplink phase, U_1 and U_2 use the energy harvested during the downlink phase to transmit their data simultaneously to the H-AP. We apply the RSMA technique to manage the uplink transmissions and mitigate interference. The transmit power available for each user in the uplink is derived from the energy harvested during the downlink phase. This is mathematically expressed as

$$p_i = \frac{\eta_i \tau_d P_A |h_i|^2}{\tau_u}, \quad i \in \{1, 2\} \quad (4)$$

where τ_u is the duration of the uplink phase.

- τ_u determines how efficiently the harvested energy is allocated for uplink transmission.
- The ratio $\frac{\tau_d}{\tau_u}$ determines how much energy is allocated for uplink transmission relative to the total harvested energy.
- Increasing τ_d results in more energy harvested, but it also reduces the available time for data transmission, creating a trade-off.

This equation highlights the fundamental trade-off between energy harvesting and data transmission duration, which is a critical aspect of system design in WPCNs. For further details on similar optimization frameworks, refer to [15]. We split the messages of U_1 and U_2 denoted as x_1 and x_2 , respectively, into two sub-messages that are independently encoded into streams $\{s_{11}, s_{12}\}$ and $\{s_{21}, s_{22}\}$. These streams are then assigned specific power levels and superposed at U_1 and U_2 . The received power at the H-AP is determined by the transmit power of each user and their respective channel gains. Since each user transmits a superposition of sub-messages in the uplink, the received signal at the H-AP is given by

$$y_A = \sqrt{\alpha_1 p_1 h_1} s_{11} + \sqrt{(1 - \alpha_1) p_1 h_1} s_{12} + \sqrt{\alpha_2 p_2 h_2} s_{21} + \sqrt{(1 - \alpha_2) p_2 h_2} s_{22} + z_A, \quad (5)$$

where the equation elements are defined as follows:

- p_1 and p_2 are the transmit powers of U_1 and U_2 , respectively, which depend on the harvested energy.
- h_1 and h_2 are the respective channel coefficients of the users.
- $0 \leq \alpha_1, \alpha_2 \leq 1$ control the sub-messages.

- z_A represents the additive white Gaussian noise at the H-AP with zero mean and variance σ^2 .
- $s_j, j \in \{11, 12, 21, 22\}$ satisfies $\mathbb{E}[|s_j|^2] = 1$.

The received power at the H-AP for user U_i can be expressed as

$$P_{\text{received},i} \propto p_i |h_i|^2, \quad i \in \{1, 2\} \quad (6)$$

From this equation, it is evident that a stronger channel gain h_i leads to a higher received power at the H-AP, improving the signal decoding performance. However, due to interference and noise, optimal allocation of α_1 and α_2 is required to balance the trade-off between throughput and interference mitigation. The parameters α_1 and α_2 control the power allocation between sub-messages in the RSMA-based uplink transmission. Their values significantly impact the SINR at the H-AP, directly affecting the achievable rates of the users. To ensure an optimal trade-off between throughput and fairness, we optimize α_1 and α_2 using the SPSA algorithm. This allows dynamic adjustment of power allocation in response to changing channel conditions. Mathematically, the optimal values of α_1 and α_2 are determined as follows:

$$\{\alpha_1^*, \alpha_2^*\} = \arg \max_{\alpha_1, \alpha_2} \sum_{i=1}^2 R_i(\alpha_1, \alpha_2) \quad (7)$$

where R_i represents the achievable rate for user U_i , and the constraints $0 \leq \alpha_1, \alpha_2 \leq 1$ ensure feasible power allocation. The SPSA algorithm iteratively updates α_1 and α_2 based on gradient approximations, making it computationally efficient for real-time optimization. This optimization ensures efficient interference management, leading to improved SINR, fair resource distribution between sub-messages, and better adaptability to dynamic channel conditions. By jointly optimizing α_1 , α_2 , and the time allocation parameters, the RSMA-based system achieves superior performance compared to traditional schemes.

RSMA Decoding Process at the H-AP

The H-AP applies RSMA and executes the successive interference cancellation (SIC) to decode the messages in the order of $s_{11} \rightarrow s_{21} \rightarrow s_{12} \rightarrow s_{22}$. The SINR for s_{11} at the H-AP is expressed as

$$\gamma_{11} = \frac{\alpha_1 p_1 |h_1|^2}{(1 - \alpha_1) p_1 |h_1|^2 + \alpha_2 p_2 |h_2|^2 + (1 - \alpha_2) p_2 |h_2|^2 + \sigma^2} \quad (8)$$

After successfully decoding and removing s_{11} , the H-AP decodes s_{21} . The SINR of s_{21} is expressed as

$$\gamma_{21} = \frac{\alpha_2 p_2 |h_2|^2}{(1 - \alpha_1) p_1 |h_1|^2 + (1 - \alpha_2) p_2 |h_2|^2 + \sigma^2} \quad (9)$$

Similarly, after successfully decoding s_{21} and subtracting it, the SINR of s_{12} is expressed as

$$\gamma_{12} = \frac{(1 - \alpha_1) p_1 |h_1|^2}{(1 - \alpha_2) p_2 |h_2|^2 + \sigma^2} \quad (10)$$

Similarly, after successfully decoding s_{12} and subtracting it, the SINR of s_{22} is expressed as

$$\gamma_{22} = \frac{(1 - \alpha_2) p_2 |h_2|^2}{\sigma^2} \quad (11)$$

The achievable rates of users U_1 and U_2 in RSMA are computed using the Shannon capacity formula:

$$R_1 = \tau_u \log_2(1 + \gamma_{11}) + \tau_u \log_2(1 + \gamma_{12}), \quad (12)$$

$$R_2 = \tau_u \log_2(1 + \gamma_{21}) + \tau_u \log_2(1 + \gamma_{22}), \quad (13)$$

Each SINR term represents the quality of the received signal at the H-AP.

3. Problem Formulation and Network Resource Optimization

In this section, we formulate two distinct optimization problems to address critical challenges in RIS-aided RSMA-enabled WPCNs, the sum throughput optimization problem and the fairness problem. For each problem, we jointly optimize the power allocation coefficients for RSMA and the time allocation between the WET and WIT phases. These formulations aim to investigate the trade-offs between maximizing the system's sum throughput and ensuring fairness by maximizing a minimum throughput among users.

3.1. Sum Throughput Maximization Problem

In this problem, the objective is to maximize the total uplink throughput of the system by jointly optimizing the rate-splitting coefficients for the split messages and the time allocations for the downlink and uplink phases. The optimization is conducted under the constraint that all the harvested energy during the downlink phase is fully utilized for uplink communication, i.e., $p_i = \frac{\eta_i \tau_d P_A |h_i|^2}{\tau_u}$; $i \in \{1, 2\}$.

$$\mathcal{P}1 \max_{\alpha_1, \alpha_2, \tau_d, \tau_u} R_1 + R_2 \quad (14a)$$

$$\text{subject to } \tau_d + \tau_u \leq 1 \quad (14b)$$

$$0 \leq \alpha_1, \alpha_2 \leq 1 \quad (14c)$$

$$\tau_d \geq 0; \tau_u \geq 0 \quad (14d)$$

Constraint (14b) ensures that the total time allocation for the downlink (energy harvesting) and uplink (data transmission) phases does not exceed the overall time frame, normalized to 1. This enforces realistic partitioning of time resources between the two phases. Constraint (14c) ensures that it remains within feasible bounds. This parameter determines how power is divided between the split messages of U_1 in the RSMA-based uplink transmission. Finally, constraint (14d) ensures that all the optimization variables are non-negative, which aligns with practical physical limitations on time allocations.

3.2. Fairness Problem

Here, we address the fairness problem in uplink WIT. The primary objective is to maximize the minimum throughput for U_1 and U_2 , thereby ensuring fairness across the network. The optimization problem is formulated as

$$\mathcal{P}2 \max_{\alpha_1, \alpha_2, \tau_d, \tau_u} \min(R_1, R_2) \quad (15a)$$

$$\text{subject to } (14b) - (14d) \quad (15b)$$

This problem ensures balanced resource allocation while considering the limitations imposed by energy harvesting and channel conditions. The focus on fairness addresses disparities in user throughput caused by variations in channel quality and energy harvesting efficiency, promoting equitable access to network resources.

4. Simultaneous Perturbation Stochastic Approximation (SPSA)-Based Solution

$\mathcal{P}1$ and $\mathcal{P}2$ represent non-convex objective functions and include non-convex constraints, primarily due to the highly coupled optimization variables, i.e., time allocations, and the RSMA-based split power coefficients. Their non-linear inter-dependencies, combined with strict system constraints, make conventional optimization techniques impractical. Therefore, we propose utilizing the simultaneous perturbation stochastic approximation (SPSA) algorithm as a robust and efficient solution framework. SPSA is a stochastic optimization algorithm that is well suited for high-dimensional problems with noisy objective functions. Unlike gradient-based methods, SPSA estimates the gradient of the objective function using a small number of noisy measurements, making it computationally efficient and scalable. This feature is particularly advantageous for non-convex optimization problems like $\mathcal{P}1$ and $\mathcal{P}2$, where the exact gradients are difficult to compute.

SPSA operates by approximating the gradient of the objective function $L(\mathbf{x})$ using stochastic perturbations. Unlike traditional gradient-based methods that require explicit derivative calculations, SPSA uses only two evaluations of the objective function per iteration, irrespective of the number of optimization variables. This makes it computationally efficient and scalable, particularly for non-convex problems in high-dimensional spaces.

The process begins by initializing the optimization variables:

$$\mathbf{x}_0 = [\alpha_1, \alpha_2, \tau_d, \tau_u]^T \quad (16)$$

where these variables are chosen to satisfy the system constraints. For instance, the time allocation variables τ_d and τ_u are subject to the constraint (14b). The RSMA coefficients α_1 and α_2 must satisfy (14c). These constraints ensure that all variables remain physically feasible within the operational limits of the system.

At each iteration k , SPSA estimates the gradient of the objective function using a stochastic perturbation vector:

$$\Delta_k = [\Delta_{k,1}, \Delta_{k,2}, \dots, \Delta_{k,n}]^T \quad (17)$$

where each component $\Delta_{k,i}$ is randomly drawn from a symmetric Bernoulli distribution (± 1). The objective function is evaluated at two perturbed points:

$$L_+ = L(\mathbf{x}_k + c_k \Delta_k), \quad L_- = L(\mathbf{x}_k - c_k \Delta_k) \quad (18)$$

where c_k is a perturbation constant that scales the perturbations. The gradient is then approximated as

$$\hat{\mathbf{g}}_k = \frac{L_+ - L_-}{2c_k} \cdot \Delta_k^{-1} \quad (19)$$

where Δ_k^{-1} denotes the element-wise inverse of the perturbation vector. This estimated gradient guides the iterative update of the optimization variables as follows:

$$\mathbf{x}_{k+1} = \mathbf{x}_k - a_k \hat{\mathbf{g}}_k \quad (20)$$

where a_k is the step size, defined as

$$a_k = \frac{a}{(A + k)^\gamma} \quad (21)$$

with $a, A, \gamma > 0$ being tunable parameters. This step size decreases over iterations to ensure convergence. To maintain feasibility, the updated variables are projected back onto the constrained region defined by the system's physical and operational limits.

The stochastic perturbations in SPSA introduce randomness that allows the algorithm to explore the solution space effectively, avoiding local optima. As the algorithm progresses, the step size reduces, refining the search and ensuring convergence to a near-optimal solution. The termination criteria are based on either the stability of the objective function,

$$|L(\mathbf{x}_{k+1}) - L(\mathbf{x}_k)| < \epsilon \quad (22)$$

or reaching a maximum number of iterations. These conditions ensure computational efficiency while achieving high-quality solutions.

The application of SPSA to RSMA-enabled WPCNs offers several advantages. The proposed method summarized in Algorithm 1 efficiently handles the coupled, non-linear nature of the optimization variables, balancing system throughput and fairness. Its stochastic nature makes it robust to noise and fluctuations in channel conditions, which are inherent in wireless networks. Additionally, its low computational cost makes it practical for real-time implementation in dynamic environments.

Algorithm 1 Proposed solution based on SPSA for solving $\mathcal{P}1$ and $\mathcal{P}2$

- 1: **Input:** Objective function $L(\mathbf{x})$, initial values $\mathbf{x}_0 = [\alpha_1, \alpha_2, \tau_d, \tau_u]^T$, step size schedule a_k , perturbation scale c_k , maximum iterations k_{\max} , tolerance ϵ .
- 2: **Initialization:** Set iteration $k = 0$. Initialize \mathbf{x}_k within feasible bounds:

$$0 \leq \tau_d + \tau_u \leq 1, \quad 0 \leq \alpha_1, \alpha_2 \leq 1.$$

- 3: **while** $k < k_{\max}$ and $|L(\mathbf{x}_{k+1}) - L(\mathbf{x}_k)| \geq \epsilon$ **do**
- 4: Generate a random perturbation vector $\Delta_k = [\Delta_{k,1}, \Delta_{k,2}, \dots, \Delta_{k,n}]^T$, where $\Delta_{k,i} \sim \{-1, 1\}$.
- 5: Compute perturbed objective function values:

$$L_+ = L(\mathbf{x}_k + c_k \Delta_k), \quad L_- = L(\mathbf{x}_k - c_k \Delta_k).$$

- 6: Estimate the gradient:

$$\hat{g}_k = \frac{L_+ - L_-}{2c_k} \cdot \Delta_k^{-1},$$

where Δ_k^{-1} denotes the element-wise inverse of Δ_k .

- 7: Update the optimization variables:

$$\mathbf{x}_{k+1} = \mathbf{x}_k - a_k \hat{g}_k,$$

with $a_k = \frac{a}{(A+k)^\gamma}$, where $a, A, \gamma > 0$ are tunable parameters.

- 8: Project \mathbf{x}_{k+1} onto the feasible region:

$$0 \leq \tau_d + \tau_u \leq 1, \quad 0 \leq \alpha_1, \alpha_2 \leq 1.$$

- 9: Increment iteration counter: $k = k + 1$.

10: **end while**

11: **Output:** Optimized variables $\mathbf{x}^* = \mathbf{x}_k$.

5. Simulation Results and Discussion

To validate the proposed RSMA-aided optimization framework for WPCNs, simulations were performed under realistic and practical system settings. The channel model adopted is Rayleigh fading, capturing the random nature of wireless propagation. U_1 and U_2 are deployed at distances of 100 m and 200 m, respectively, from the hybrid access

point (H-AP). The channel incorporates path loss effects with a path loss coefficient of 3, simulating the attenuation experienced over a distance. The H-AP transmits with a fixed power of 30 dBm during the downlink phase, while the noise variance is set at -100 dBm to model typical environmental noise in wireless communication systems.

The proposed optimization framework leverages the SPSA algorithm to address the non-convex nature of the resource allocation problem. The key parameters for the SPSA algorithm were configured as perturbation size, $c = 0.1$, ensuring the perturbations remain small and controlled for efficient gradient estimation. The step size decay parameters $\gamma = 0.602$ define the rate of decay for the step size, balancing convergence speed and accuracy. The initial step size was $a = 0.002$, providing a stable starting point for iterative updates in the optimization process. The simulations were designed to evaluate the performance of the RSMA-aided solution in terms of key metrics such as sum throughput and fairness. Comparisons were made against benchmark schemes as follows:

- RSMA (Rate-Splitting Multiple Access):
RSMA shows the proposed scheme where the power allocation coefficients and time allocation for the users are both optimized using the SPSA algorithm.
- FPRSMA (Fixed Power RSMA):
FPRSMA is a variation of RSMA where the power allocation coefficients for the users are fixed and equally divided ($\alpha_1 = 0.5$, $\alpha_2 = 0.5$). However, the time allocation is dynamically optimized using the SPSA algorithm to maximize system performance.
- NONRSMA (Non-RSMA, Time-Division Multiple Access):
NONRSMA represents a scheme that adopts a time-division multiple access (TDMA) approach for uplink data transmission. In this scheme, time allocation between users is optimized using SPSA, but RSMA principles (e.g., power splitting) are not employed.
- OMA (Orthogonal Multiple Access):
OMA represents a fully orthogonal scheme where time allocation is fixed and predefined. Unlike the other schemes, OMA does not incorporate SPSA-based optimization, serving as a baseline for comparison.

Figure 2 depicts the convergence behavior of the proposed SPSA-based optimization algorithm under two different transmit power levels of the H-AP. The results demonstrate that the algorithm converges efficiently within approximately 50 iterations for both transmit power levels, reflecting the effectiveness of the SPSA method in addressing non-convex optimization problems. For $P_t = 40$ dBm, the objective function stabilizes at approximately 13.5 bps/Hz, while for $P_t = 30$ dBm, it converges to around 12 bps/Hz. This illustrates the significant impact of increased transmit power on achievable throughput, with higher power enabling better network performance. The proposed algorithm's rapid convergence and stable results confirm its robustness in optimizing resource allocation in RSMA-aided wireless powered communication networks.

Figure 3 shows the solution to $\mathcal{P}1$ and demonstrates the relationship between the sum throughput (in bps/Hz) and the transmit power of the H-AP (in dBm) for four different schemes, RSMA- $\mathcal{P}1$, FPRSMA- $\mathcal{P}1$, NONRSMA- $\mathcal{P}1$, and OMA. The results highlight the superior performance of RSMA- $\mathcal{P}1$, which involves optimizing both power allocation coefficients and time allocation using the SPSA algorithm. FPRSMA- $\mathcal{P}1$, using fixed power allocation and time optimization, achieves slightly lower throughput. NONRSMA- $\mathcal{P}1$, a TDMA-based scheme with optimized time allocation, performs moderately but remains significantly below RSMA-based schemes. OMA, with fixed power and time allocations, consistently achieves the lowest throughput. The figure demonstrates that as the H-AP transmit power increases, all schemes experience improved throughput. However, RSMA- $\mathcal{P}1$ outperforms the others significantly, showcasing the effectiveness of RSMA-based optimization in improving system performance under varying power levels.

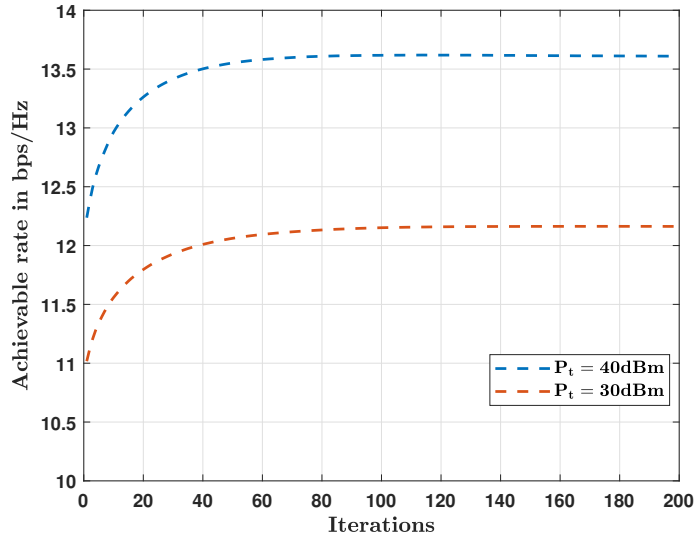


Figure 2. Convergence of proposed SPSA-based algorithm for different transmit power levels.

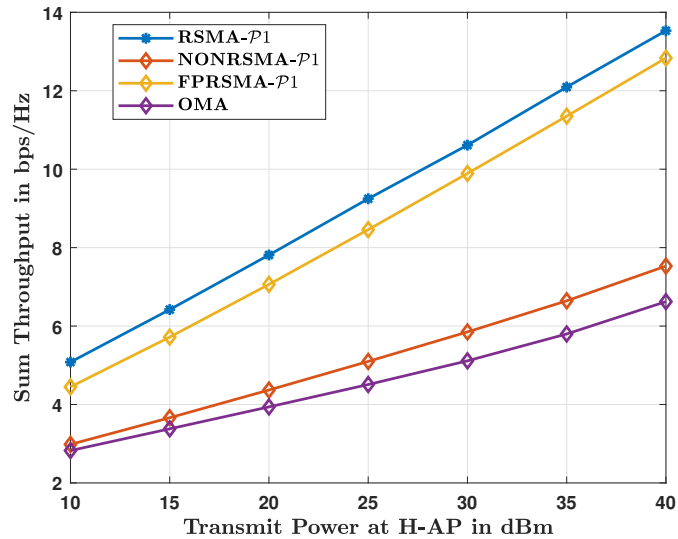


Figure 3. Sum throughput versus transmit power at H-AP for different schemes.

Figure 4 illustrates the throughput of U_2 (in bps/Hz) as a function of the transmit power of the H-AP (in dBm) for $\mathcal{P}1$ and $\mathcal{P}2$. RSMA- $\mathcal{P}1$ optimizes the sum throughput of the system, achieving a steady increase in U_2 's throughput as the transmit power grows. RSMA- $\mathcal{P}2$, which optimizes the minimum throughput to enhance fairness between users, significantly improves U_2 's throughput, particularly at higher power levels, surpassing RSMA- $\mathcal{P}1$. This demonstrates the effectiveness of RSMA- $\mathcal{P}2$ in ensuring balanced resource allocation between users. In comparison, NONRSMA- $\mathcal{P}1$, a TDMA-based scheme focused on sum throughput optimization, shows limited improvement in U_2 's throughput, reflecting the inefficiency of non-RSMA schemes in managing interference and allocating resources effectively. NONRSMA- $\mathcal{P}2$, which optimizes the minimum throughput for fairness in TDMA, provides better throughput for U_2 than NONRSMA- $\mathcal{P}1$ but remains significantly below the RSMA-based schemes, particularly at higher transmit power levels. The figure highlights the superiority of RSMA-based schemes over NONRSMA schemes in improving U_2 's performance. RSMA- $\mathcal{P}2$, in particular, demonstrates remarkable fairness by ensuring higher throughput for U_2 , even as the system prioritizes minimum throughput optimization.

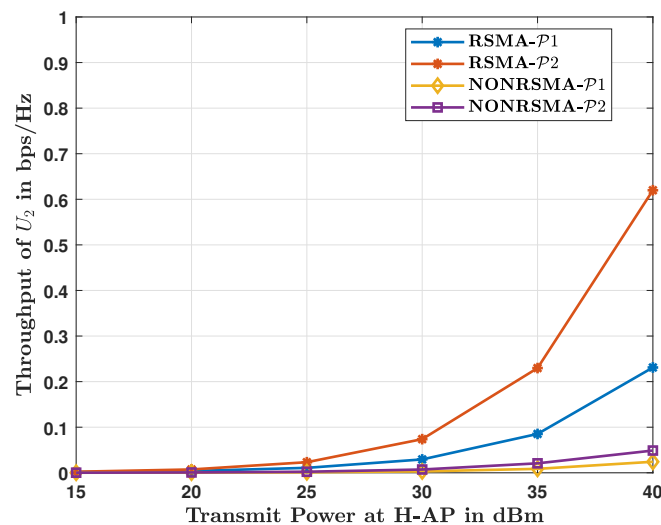


Figure 4. Throughput of U_2 versus transmit power at H-AP for different schemes.

Figure 5 illustrates the sum throughput (in bps/Hz) as a function of the distance between U_1 and U_2 (in meters). RSMA- $\mathcal{P}1$ achieves the highest and most consistent throughput, demonstrating its efficiency in handling interference and resource allocation regardless of user distance. FPRSMA also maintains a nearly constant throughput but performs slightly worse due to fixed power allocation. NONRSMA- $\mathcal{P}1$ shows a decreasing trend as distance increases, reflecting its limited ability to manage interference and adapt resource allocation. OMA performs the worst, with significant throughput degradation, as orthogonal resource allocation and fixed scheduling fail to handle the challenges of increasing user separation. The figure highlights the robust performance of RSMA- $\mathcal{P}1$ compared to other schemes.

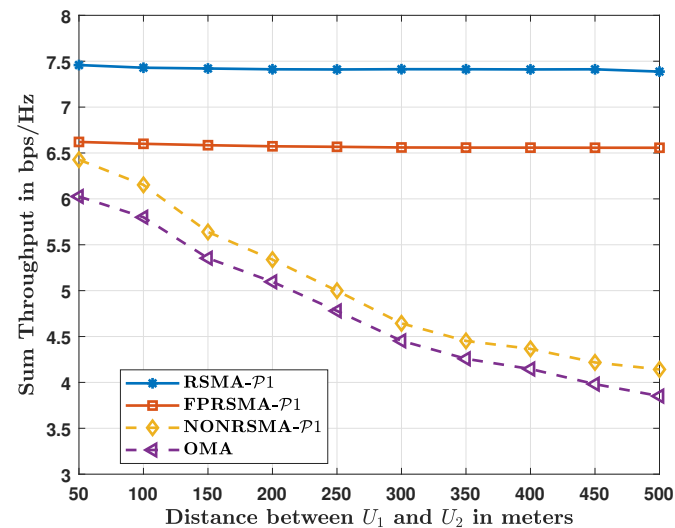


Figure 5. Sum throughput versus distance between U_1 and U_2 for different schemes.

Figure 6 illustrates the throughput of U_2 (in bps/Hz) as a function of the distance between U_1 and U_2 (in meters) for four schemes: RSMA- $\mathcal{P}1$, RSMA- $\mathcal{P}2$, NONRSMA- $\mathcal{P}1$, and NONRSMA- $\mathcal{P}2$. As the distance between users increases, the throughput of U_2 decreases across all schemes due to increased path loss and weakened interference management. RSMA- $\mathcal{P}1$ achieves the highest throughput for U_2 at shorter distances, while RSMA- $\mathcal{P}2$ performs better at larger distances, prioritizing fairness and balancing resource allocation. NONRSMA- $\mathcal{P}1$ and NONRSMA- $\mathcal{P}2$ exhibit significant degradation in

throughput with increasing distance, reflecting the limitations of TDMA-based approaches in handling interference and optimizing resource allocation. These results emphasize the superiority of RSMA in maintaining higher throughput and fairness under varying user separations.

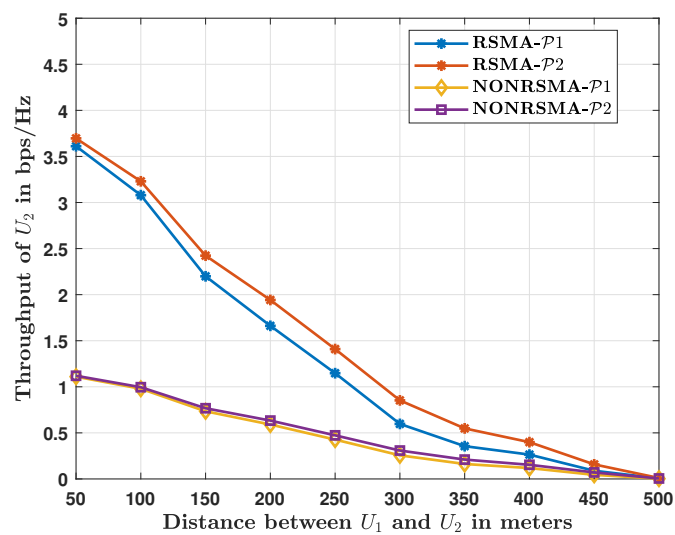


Figure 6. Throughput of U_2 versus distance between U_1 and U_2 for different schemes.

Figure 7 illustrates the sum throughput (in bps/Hz) as a function of the transmit power at the H-AP (in dBm). RSMA- $\mathcal{P}1$, which optimizes the sum throughput, achieves the highest performance across all transmit power levels, highlighting its efficiency in resource allocation and interference management. In contrast, RSMA- $\mathcal{P}2$, which focuses on maximizing the minimum throughput for fairness, provides slightly lower overall throughput but ensures better resource distribution among users, particularly benefiting those with weaker channel conditions. NONRSMA- $\mathcal{P}1$ and NONRSMA- $\mathcal{P}2$, representing TDMA-based schemes, perform significantly worse due to their limited ability to handle interference and allocate resources effectively. The trade-off between $\mathcal{P}1$ and $\mathcal{P}2$ reflects opposing objectives: $\mathcal{P}1$ maximizes efficiency but sacrifices fairness, while $\mathcal{P}2$ prioritizes fairness at the cost of reduced overall throughput. These results emphasize the superiority of RSMA schemes in achieving higher sum throughput and balancing the trade-off between fairness and efficiency.

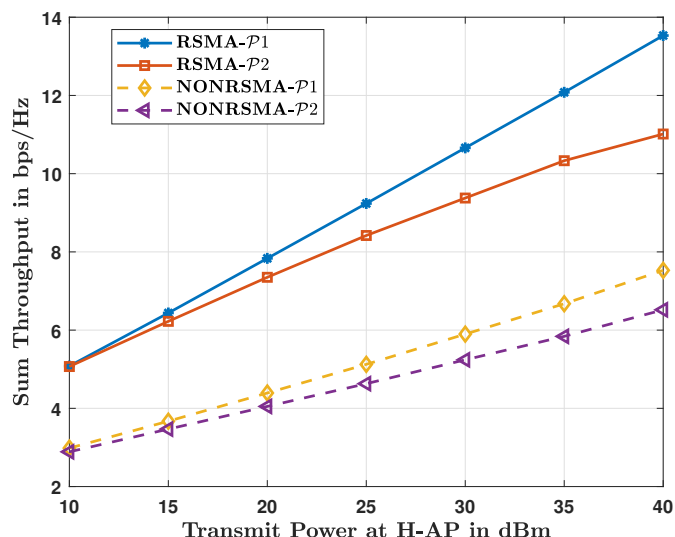


Figure 7. Sum throughput versus transmit power at H-AP.

6. Conclusions

In this paper, we proposed a novel RSMA-aided framework for WPCNs to address the dual challenges of energy efficiency and interference management in uplink communications. By integrating RSMA into the WIT phase and optimizing resource allocation jointly with WET, we investigated two key optimization problems: sum throughput maximization and fairness optimization. These non-convex problems were effectively addressed using the SSPSA method, which proved efficient in handling the complex joint optimization of rate-splitting factors and time allocation. Our numerical results demonstrated the trade-offs between the two objectives, highlighting RSMA's capability to achieve both high spectral efficiency and fairness under practical WPCN settings. Furthermore, the simulations validated RSMA's superior performance over traditional multiple-access schemes in terms of throughput, fairness, and energy efficiency. These findings establish the potential of RSMA as a promising approach for enhancing WPCN performance, paving the way for its adoption in next-generation wireless networks, especially in energy-constrained scenarios. Future work could explore extending this framework to multi-user and multi-antenna WPCNs, as well as investigating adaptive RSMA strategies for real-time resource allocation under dynamic network conditions.

Author Contributions: Conceptualization, I.H. and M.R.C.; Formal Analysis, I.H., M.A.S.S. and H.K.S.; Methodology, I.H., M.A.S.S. and M.R.C.; Supervision, H.K.S.; Validation, I.H., M.R.C. and M.A.S.S.; Writing—Original Draft, I.H. and M.A.S.S.; Writing—Review and Editing, I.H., M.R.C., M.A.S.S. and H.K.S.; Funding Acquisition, H.K.S. All authors have read and agreed to the published version of the manuscript.

Funding: This work was supported in part by an Institute of Information and Communications Technology Planning and Evaluation (IITP) grant funded by the Korean Government (Ministry of Science and ICT (MSIT), South Korea); in part under the Metaverse Support Program to Nurture the Best Talents, Grant IITP-2024-RS-2023-00254529; in part by the Basic Science Research Program through the National Research Foundation of Korea (NRF) funded by the Ministry of Education under Grant 2020R1A6A1A03038540; and in part by the MSIT (Ministry of Science and ICT, Korea) under the ITRC (Information Technology Research Center) support program (IITP-2025-RS-2024-00438007) supervised by the IITP (Institute for Information and Communications Technology Planning and Evaluation).

Data Availability Statement: The data are contained within the article.

Conflicts of Interest: The authors declare that they have no conflicts of interest regarding the publication of this paper.

References

1. Kamath, S.; Anand, S.; Buchke, S.; Agnihotri, K. A Review of Recent Developments in 6G Communications Systems. *Eng. Proc.* **2023**, *59*, 167. [[CrossRef](#)]
2. Rojek, I.; Kotlarz, P.; Dorożyński, J.; Mikołajewski, D. Sixth-Generation (6G) Networks for Improved Machine-to-Machine (M2M) Communication in Industry 4.0. *Electronics* **2024**, *13*, 1832. [[CrossRef](#)]
3. Zhang, Z.; Xiao, Y.; Ma, Z.; Xiao, M.; Ding, Z.; Lei, X.; Karagiannidis, G.K.; Fan, P. 6G Wireless Networks: Vision, Requirements, Architecture, and Key Technologies. *IEEE Veh. Technol. Mag.* **2019**, *14*, 28–41. [[CrossRef](#)]
4. Tataria, H.; Shafi, M.; Molisch, A.F.; Dohler, M.; Sjöland, H.; Tufvesson, F. 6G Wireless Systems: Vision, Requirements, Challenges, Insights, and Opportunities. *Proc. IEEE* **2021**, *109*, 1166–1199. [[CrossRef](#)]
5. Guo, F.; Yu, F.R.; Zhang, H.; Li, X.; Ji, H.; Leung, V.C.M. Enabling Massive IoT Toward 6G: A Comprehensive Survey. *IEEE Internet Things J.* **2021**, *8*, 11891–11915. [[CrossRef](#)]
6. Zhang, H.; Shlezinger, N.; Guidi, F.; Dardari, D.; Imani, M.F.; Eldar, Y.C. Near-Field Wireless Power Transfer for 6G Internet of Everything Mobile Networks: Opportunities and Challenges. *IEEE Commun. Mag.* **2022**, *60*, 12–18. [[CrossRef](#)]
7. Verma, S.; Kaur, S.; Khan, M.A.; Sehdev, P.S. Toward Green Communication in 6G-Enabled Massive Internet of Things. *IEEE Internet Things J.* **2021**, *8*, 5408–5415. [[CrossRef](#)]

8. Lu, X.; Wang, P.; Niyato, D.; Kim, D.I.; Han, Z. Wireless Networks with RF Energy Harvesting: A Contemporary Survey. *IEEE Commun. Surv. Tutor.* **2015**, *17*, 757–789. [\[CrossRef\]](#)
9. Bi, S.; Zeng, Y.; Zhang, R. Wireless powered communication networks: An overview. *IEEE Wirel. Commun.* **2016**, *23*, 10–18. [\[CrossRef\]](#)
10. Bi, S.; Ho, C.K.; Zhang, R. Wireless powered communication: Opportunities and challenges. *IEEE Commun. Mag.* **2015**, *53*, 117–125. [\[CrossRef\]](#)
11. Ramezani, P.; Jamalipour, A. Toward the Evolution of Wireless Powered Communication Networks for the Future Internet of Things. *IEEE Netw.* **2017**, *31*, 62–69. [\[CrossRef\]](#)
12. Jamshed, M.A.; Ali, K.; Abbasi, Q.H.; Imran, M.A.; Ur-Rehman, M. Challenges, Applications, and Future of Wireless Sensors in Internet of Things: A Review. *IEEE Sens. J.* **2022**, *22*, 5482–5494. [\[CrossRef\]](#)
13. Moloudian, G.; Hosseinfard, M.; Kumar, S.; Simorangkir, R.B.V.B.; Buckley, J.L.; Song, C.; Fantoni, G.; O’Flynn, B. RF Energy Harvesting Techniques for Battery-Less Wireless Sensing, Industry 4.0, and Internet of Things: A Review. *IEEE Sens. J.* **2024**, *24*, 5732–5745. [\[CrossRef\]](#)
14. Liu, X.; Qin, Z.; Gao, Y.; McCann, J.A. Resource Allocation in Wireless Powered IoT Networks. *IEEE Internet Things J.* **2019**, *6*, 4935–4945. [\[CrossRef\]](#)
15. Ju, H.; Zhang, R. Throughput Maximization in Wireless Powered Communication Networks. *IEEE Trans. Wirel. Commun.* **2014**, *13*, 418–428. [\[CrossRef\]](#)
16. Zhang, L.; Liang, Y.C.; Niyato, D. 6G Visions: Mobile ultra-broadband, super internet-of-things, and artificial intelligence. *China Commun.* **2019**, *16*, 1–14. [\[CrossRef\]](#)
17. Zhang, M.; Shen, L.; Ma, X.; Liu, J. Toward 6G-Enabled Mobile Vision Analytics for Immersive Extended Reality. *IEEE Wirel. Commun.* **2023**, *30*, 132–138. [\[CrossRef\]](#)
18. Zawish, M.; Dharejo, F.A.; Khowaja, S.A.; Raza, S.; Davy, S.; Dev, K.; Bellavista, P. AI and 6G Into the Metaverse: Fundamentals, Challenges and Future Research Trends. *IEEE Open J. Commun. Soc.* **2024**, *5*, 730–778. [\[CrossRef\]](#)
19. Clerckx, B.; Joudeh, H.; Hao, C.; Dai, M.; Rassouli, B. Rate splitting for MIMO wireless networks: A promising PHY-layer strategy for LTE evolution. *IEEE Commun. Mag.* **2016**, *54*, 98–105. [\[CrossRef\]](#)
20. Mao, Y.; Dizdar, O.; Clerckx, B.; Schober, R.; Popovski, P.; Poor, H.V. Rate-Splitting Multiple Access: Fundamentals, Survey, and Future Research Trends. *IEEE Commun. Surv. Tutor.* **2022**, *24*, 2073–2126. [\[CrossRef\]](#)
21. Mishra, A.; Mao, Y.; Dizdar, O.; Clerckx, B. Rate-Splitting Multiple Access for 6G—Part I: Principles, Applications and Future Works. *IEEE Commun. Lett.* **2022**, *26*, 2232–2236. [\[CrossRef\]](#)
22. Clerckx, B.; Mao, Y.; Schober, R.; Poor, H.V. Rate-Splitting Unifying SDMA, OMA, NOMA, and Multicasting in MISO Broadcast Channel: A Simple Two-User Rate Analysis. *IEEE Wirel. Commun. Lett.* **2020**, *9*, 349–353. [\[CrossRef\]](#)
23. Liu, L.; Zhang, R.; Chua, K. Multi-Antenna Wireless Powered Communication with Energy Beamforming. *IEEE Trans. Commun.* **2014**, *62*, 4349–4361. [\[CrossRef\]](#)
24. Hameed, I.; Tuan, P.V.; Camana, M.R.; Koo, I. Optimal Energy Beamforming to Minimize Transmit Power in a Multi-Antenna Wireless Powered Communication Network. *Electronics* **2021**, *10*, 509. [\[CrossRef\]](#)
25. Wang, D.; Tellambura, C. Performance Analysis of Energy Beamforming WPCN Links with Channel Estimation Errors. *IEEE Open J. Commun. Soc.* **2020**, *1*, 1153–1170. [\[CrossRef\]](#)
26. Song, D.; Shin, W.; Lee, J.; Poor, H.V. Sum-Throughput Maximization in NOMA-Based WPCN: A Cluster-Specific Beamforming Approach. *IEEE Internet Things J.* **2021**, *8*, 10543–10556. [\[CrossRef\]](#)
27. Khazali, A.; Tarchi, D.; Shayesteh, M.G.; Kalbkhani, H.; Bozorgchenani, A. Energy Efficient Uplink Transmission in Cooperative mmWave NOMA Networks with Wireless Power Transfer. *IEEE Trans. Veh. Technol.* **2022**, *71*, 391–405. [\[CrossRef\]](#)
28. Liu, Y.; Na, Z.; Liu, A.; Deng, Z. A Hybrid Multiple Access Scheme in Wireless Powered Communication Systems. In *Communications, Signal Processing, and Systems, Proceedings of the 8th International Conference on Communications, Signal Processing, and Systems, Urumqi, China, 20–22 July 2019*; Liang, Q., Wang, W., Liu, X., Na, Z., Jia, M., Zhang, B., Eds.; Springer: Singapore, 2020; pp. 1528–1532.
29. Afridi, A.; Hameed, I.; García, C.E.; Koo, I. Throughput Maximization of Wireless Powered IoT Network with Hybrid NOMA-TDMA Scheme: A Genetic Algorithm Approach. *IEEE Access* **2024**, *12*, 65241–65253. [\[CrossRef\]](#)
30. Mao, Y.; Clerckx, B.; Li, V.O. Rate-Splitting for Multi-User Multi-Antenna Wireless Information and Power Transfer. In *Proceedings of the 2019 IEEE 20th International Workshop on Signal Processing Advances in Wireless Communications (SPAWC)*, Cannes, France, 2–5 July 2019; pp. 1–5. [\[CrossRef\]](#)
31. Camana Acosta, M.R.; Moreta, C.E.G.; Koo, I. Joint Power Allocation and Power Splitting for MISO-RSMA Cognitive Radio Systems with SWIPT and Information Decoder Users. *IEEE Syst. J.* **2021**, *15*, 5289–5300. [\[CrossRef\]](#)
32. Camana, M.R.; Garcia, C.E.; Koo, I. Rate-Splitting Multiple Access in a MISO SWIPT System Assisted by an Intelligent Reflecting Surface. *IEEE Trans. Green Commun. Netw.* **2022**, *6*, 2084–2099. [\[CrossRef\]](#)

33. Abbasi, O.; Yanikomeroglu, H. Transmission Scheme, Detection and Power Allocation for Uplink User Cooperation with NOMA and RSMA. *IEEE Trans. Wirel. Commun.* **2023**, *22*, 471–485. [[CrossRef](#)]
34. Khisa, S.; Elhattab, M.; Arfaoui, M.A.; Sharafeddine, S.; Assi, C. Power Allocation and Beamforming Design for Uplink Rate-Splitting Multiple Access with User Cooperation. *IEEE Trans. Veh. Technol.* **2024**, *73*, 10738–10743. [[CrossRef](#)]
35. Xiao, F.; Wen, M.; Yang, L.; Tsiftsis, T.A.; Liu, H. Intelligent Rate-Splitting Multiple Access-Enabled Coordinated Direct and Relay Transmission. *IEEE Wirel. Commun. Lett.* **2024**, *13*, 2606–2610. [[CrossRef](#)]

Disclaimer/Publisher’s Note: The statements, opinions and data contained in all publications are solely those of the individual author(s) and contributor(s) and not of MDPI and/or the editor(s). MDPI and/or the editor(s) disclaim responsibility for any injury to people or property resulting from any ideas, methods, instructions or products referred to in the content.